Complex Dielectric Measurements and Analysis of Brain Tissues in the Radio and Microwave Frequencies

Jian-Zhong Bao, *Senior Member, IEEE,* Shin-Tsu Lu, and William D. Hurt, *Senior Member, IEEE*

***Abstract*—We present *in-vitro* complex dielectric measurements of gray and white matter of rat brains in the frequency range between 45 MHz and 26.5 GHz at body and room temperatures using the open-ended coaxial probe technique with an HP8510B network analyzer. The measurement data exhibited two separated dispersions, and were analyzed by means of a complex nonlinear least-squares technique. We suggest two empirical models to describe the experimental data: one containing two Cole–Cole functions was applied to the data from this paper, and another including one Havriliak–Negami and one Cole–Cole function was utilized to a combination of past and present literature data in a wider frequency range from 100 kHz to 26.5 GHz. The adoption of previously published data at the frequencies below 45 MHz increases the valid frequency range of the model.**

***Index Terms*—Brain tissues, complex dielectric constant, complex nonlinear modeling, open-ended coaxial probe technique, radio and microwave frequencies.**

I. Introduction

THE lack of sufficient data at super-high frequencies and accurate models in a wide frequency range for complex dielectric properties of tissues has presented an obstacle for both theoretical and experimental studies of electromagnetic energy deposition in human or animal bodies. Most of the early studies were at a few discrete frequency bands or scattered frequency points, and in frequencies below 5 GHz. There are also very few published data above 10 GHz, and virtually no model covers a wide frequency range [1]–[3]. It is important to establish a reliable database and empirical models for each organ in a wide frequency range for studies of the interaction between electromagnetic wave and biological bodies [4], especially for pulse situations. The dielectric information is also of importance for clinical applications [5].

In this paper, we report *in-vitro* complex dielectric measurements of gray and white matter from rat brains in the frequency range between 45 MHz and 26.5 GHz using the open-ended coaxial probe technique with a computer-controlled HP8510B network analyzer and the complex nonlinear modeling of experimental data. The measurements were performed at 37 °C

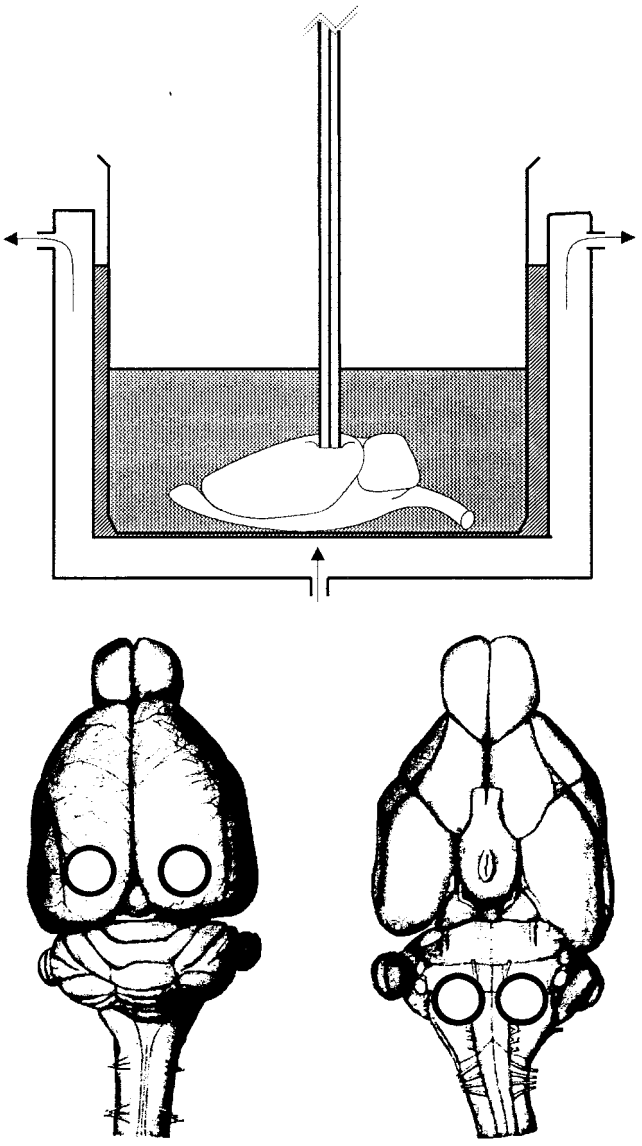

(a) (b)

Fig. 1. Tissue and probe configuration and measurement locations on the surface of a rat brain. The circles indicate the locations on the (a) cerebral cortex for gray matter and on the (b) medulla oblongata for white matter measurements.

Manuscript received February 27, 1997; revised June 20, 1997. This work was supported by the U.S. Army Medical Research and Materiel Command under Contract DAMD17-94-C-4069 awarded to McKesson BioServices.

J.-Z. Bao is with McKesson BioServices and the U.S. Army Medical Research Detachment, Brooks Air Force Base, San Antonio, TX 78235 USA (e-mail: jian@abba.brooks.af.mil).

S.-T. Lu is with McKesson BioServices and the U.S. Army Medical Research Detachment, Brooks Air Force Base, San Antonio, TX 78235 USA.

W. D. Hurt is with Armstrong Laboratory, Brooks Air Force Base, San Antonio, TX 78235 USA.

Publisher Item Identifier S 0018-9480(97)07109-3.

TABLE I
BEST-FITTED PARAMETERS IN (3) FOR THE GRAY AND WHITE MATTER OF RAT BRAINS AT ROOM AND BODY TEMPERATURES. THE CORRESPONDING COMPARISONS BETWEEN THE EXPERIMENTAL DATA AND THEIR FITTING ARE IN FIGS. 5 AND 6

	gray matter		white matter	
	24 °C	37 °C	25 °C	37 °C
$\Delta\epsilon_1$	269.7 ± 2.6	309.8 ± 7.8	110.4 ± 6.6	130.3 ± 9.1
τ_1 (ns)	5.59 ± 0.04	5.12 ± 0.11	6.24 ± 0.35	5.31 ± 0.40
α_1	0.910 ± 0.003	0.892 ± 0.026	0.840 ± 0.005	0.806 ± 0.007
$\Delta\epsilon_2$	50.26 ± 0.04	46.68 ± 0.11	31.19 ± 0.14	28.12 ± 0.16
τ_2 (ps)	6.74 ± 0.06	4.87 ± 0.12	5.20 ± 0.22	3.04 ± 0.17
α_2	0.907 ± 0.002	0.939 ± 0.004	0.732 ± 0.059	0.760 ± 0.007
ϵ_h	5.11 ± 0.02	4.54 ± 0.04	4.79 ± 0.02	4.40 ± 0.03
σ_0 (S/m)	0.366 ± 0.002	0.368 ± 0.005	0.234 ± 0.003	0.241 ± 0.005

and 24 °C for gray and at 37 °C and 25 °C for white matter. The measured data were analyzed with two empirical models. One of these included two Cole–Cole functions [6] and was utilized with the data from this paper to obtain a model for the frequencies between 45 MHz and 26.5 GHz. The other model contained a Havriliak–Negami [6] and a Cole–Cole function, and was applied to the combined data from this paper and results of [7], [8] at the frequencies below 45 MHz to construct a model which covers a wider frequency range between 100 kHz and 26.5 GHz. Although the first model gives a better fit to the measured spectra in general, the second one simulates the complex dielectric spectra in a much wider frequency range.

II. MEASUREMENTS

A. Open-Ended Coaxial Probe Technique

The open-ended coaxial probe technique has been extensively employed for the dielectric measurements of materials, especially biological samples [9]–[13]. With this technique, the complex dielectric spectra can be easily acquired in a wide frequency range and in an almost continuous form. The technique is especially suitable for liquids. The measurements for solids are much more tedious, and the main problem is to assure a good and tight contact between the open end of the coaxial probe and the sample surface [14], [15]. A very tiny air gap could introduce a very large error, especially to the high dielectric constant materials [16]. For soft solids such as tissues, a good contact can be realized by applying moderate pressure.

The measured complex reflection coefficient (ρ_m) contains the desired information from the interface between the open end of a probe and the material under measurement as well as the undesired effects of the network analyzer (which was not calibrated), connectors, and coaxial line. With a linear model for the interface, ρ_m can be converted to the complex relative dielectric constant ($\epsilon = \epsilon' - j\epsilon''$, where $j = \sqrt{-1}$) with [17], [18]

$$\epsilon = \frac{A_1\rho_m - A_2}{A_3 - \rho_m} \tag{1}$$

where the complex coefficients A_1, A_2, and A_3 were determined with a calibration procedure using three reference measurements: an open, a short, and standard saline. This simple rational expression maps *one* point in the complex ρ_m plane to *one* point in the complex ϵ plane. Although this relation is based on assumptions and simplifications, using standards in the calibration procedure will compensate for the measurement errors to a large extent, especially when the dielectric properties under investigation are close to one of the standards used for the calibration [18]. The advantage of (1)

TABLE II
BEST-FITTED PARAMETERS IN (4) FOR THE GRAY AND WHITE MATTER OF RAT BRAINS WITH THE ADOPTION OF EARLY PUBLISHED LOW-FREQUENCY DATA OF A DOG BRAIN. THE CORRESPONDING COMPARISONS BETWEEN THE EXPERIMENTAL DATA AND THEIR FITTING ARE IN FIGS. 7 AND 8

	gray matter		white matter	
	24 °C	37 °C	25 °C	37 °C
$\Delta\epsilon_1$	7703	9217	7961	8502
τ_1 (ns)	59.1	182.1	24.9	605.5
α_1	0.300	0.364	0.214	0.348
β_1	3.190	2.297	5.010	2.300
$\Delta\epsilon_2$	45.27	40.76	29.01	26.38
τ_2 (ps)	6.12	4.27	4.35	2.96
α_2	0.999	0.997	0.787	0.817
ϵ_h	4.92	5.18	4.55	4.81
σ_0 (S/m)	0.155	0.163	0.102	0.128

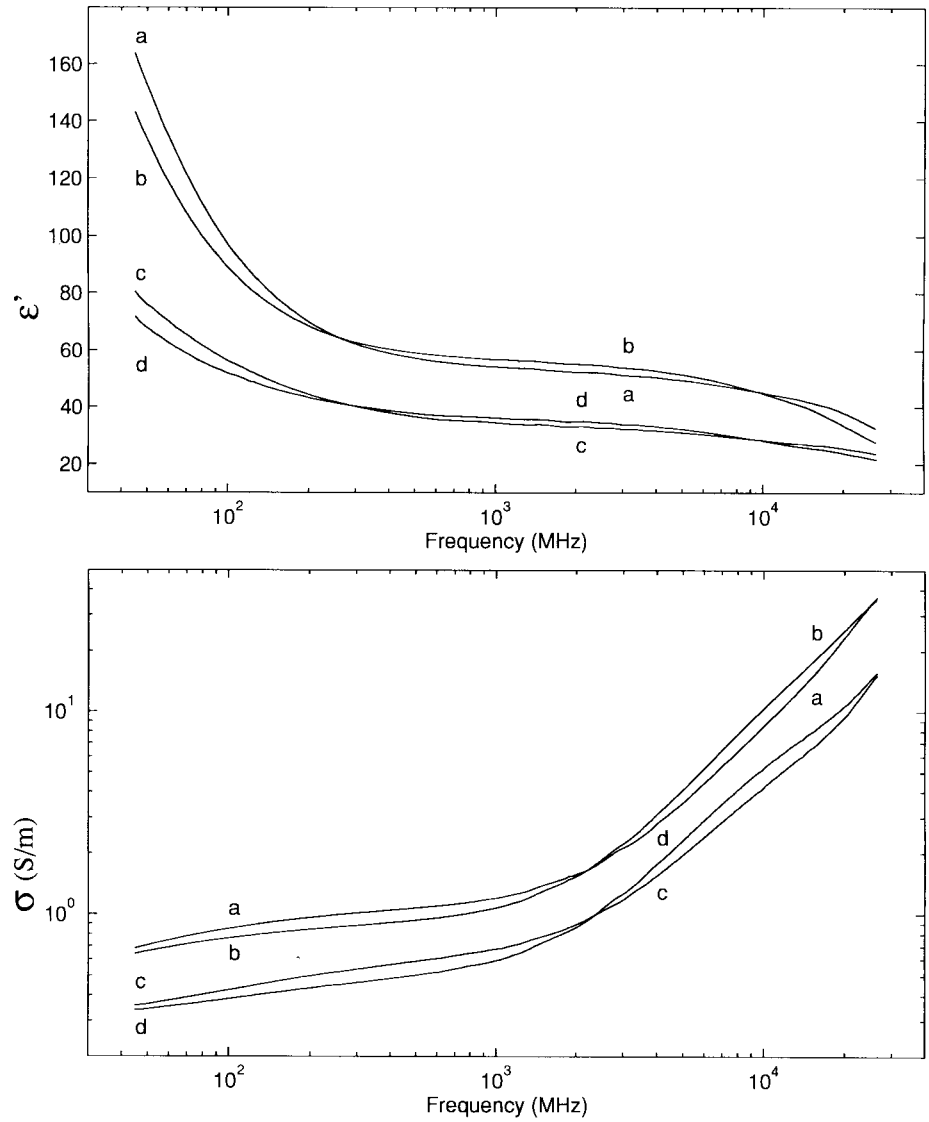

Fig. 2. Permittivity and conductivity spectra of gray matter at a: 37 ± 0.5 °C, b: 24 ± 0.5 °C; white matter at c: 37 ± 0.5 °C, and d: 25 ± 0.5 °C.

TABLE III
COMPARISON OF VALUES FROM (3) AND (4) USING THE PARAMETERS LISTED IN TABLES I AND II, RESPECTIVELY, WITH THE EXPERIMENTAL DATA FOR GRAY MATTER AT 37 °C AT SOME SELECTED FREQUENCY POINTS. THESE POINTS ARE IN CURVES a OF FIGS. 6 AND 8. THE EXPERIMENTAL DATA AT 0.1, 1, AND 10 MHz ARE FROM [1] AND [7]. N/A STANDS FOR NOT APPLICABLE

	ϵ'			σ (S/m)		
frequencies (MHz)	value of Eq. (3)	value of Eq. (4)	experimental data	value of Eq. (3)	value of Eq. (4)	experimental data
0.1	N/A	3934	3800	N/A	0.173	0.170
1.0	N/A	1570	1250	N/A	0.231	0.210
10.0	N/A	395	366 ± 14	N/A	0.427	0.365 ± 0.015
99.9	97.1	101	96.9 ± 7.0	0.851	0.798	0.850 ± 0.040
901.8	54.3	54.2	54.4 ± 3.0	1.19	1.34	1.18 ± 0.10
10179.8	45.8	44.1	45.0 ± 2.0	8.83	7.93	8.67 ± 0.85
26500.0	32.2	32.6	32.6 ± 2.3	32.1	30.7	36.7 ± 2.7

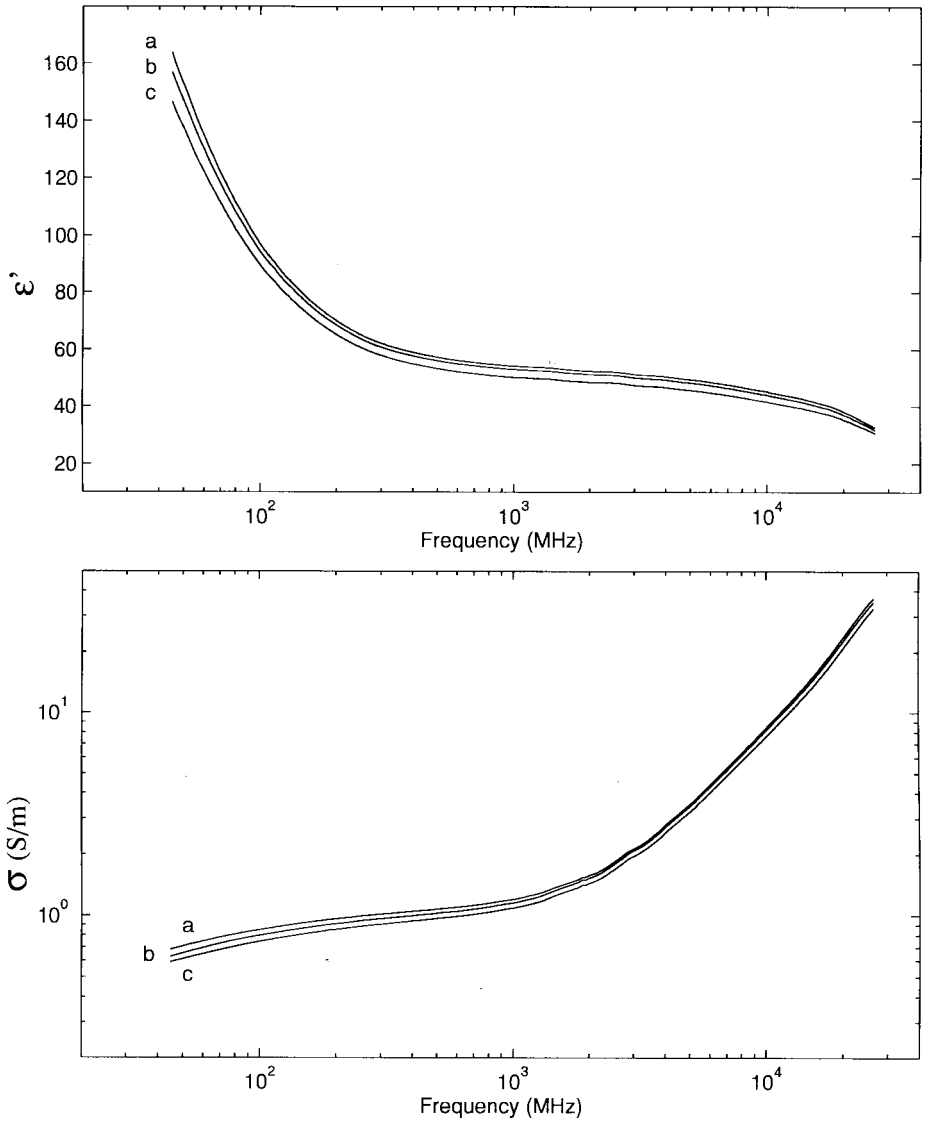

Fig. 3. The systematic time variation of the permittivity and conductivity spectra of gray matter of one typical measurement setup at a: 1 min, b: 11 min, and c: 21 min after the probe contacted the sample surface at 37 $\pm$ 0.5 °C.

TABLE IV
COMPARISON OF VALUES FROM (3) AND (4) USING THE PARAMETERS LISTED IN TABLES I AND II, RESPECTIVELY, WITH THE EXPERIMENTAL DATA FOR WHITE MATTER AT 37 °C AT SOME SELECTED FREQUENCY POINTS. THESE POINTS ARE IN CURVES b OF FIGS. 6 AND 8. THE EXPERIMENTAL DATA AT 0.1, 1, AND 10 MHz ARE FROM [1] AND [7]. N/A STANDS FOR NOT APPLICABLE

	ϵ'			σ (S/m)		
frequencies (MHz)	value of Eq. (3)	value of Eq. (4)	experimental data	value of Eq. (3)	value of Eq. (4)	experimental data
0.1	N/A	2354	2680 ± 720	N/A	0.135	0.135 ± 0.015
1.0	N/A	767.8	685 ± 142	N/A	0.168	0.165 ± 0.025
10.0	N/A	183.4	186 ± 23	N/A	0.256	0.255 ± 0.045
99.9	56.9	56.1	56.1 ± 5.0	0.433	0.416	0.425 ± 0.042
901.8	34.9	35.0	34.9 ± 2.0	0.682	0.692	0.662 ± 0.075
10179.8	28.8	28.7	28.3 ± 1.5	4.17	4.07	4.32 ± 0.57
26500.0	23.7	23.8	23.7 ± 1.5	13.8	14.0	15.2 ± 1.5

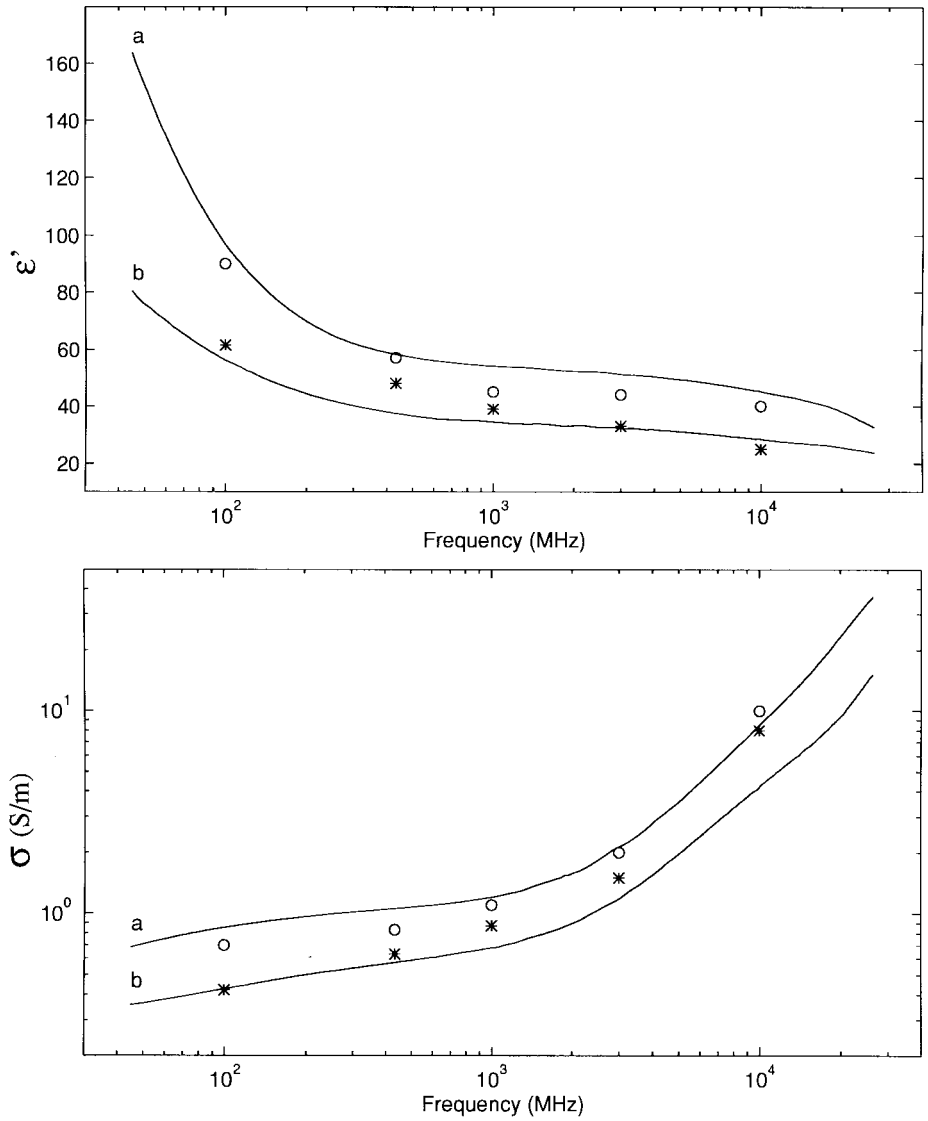

Fig. 4. Comparison of permittivity and conductivity spectra of rat brain tissues between this paper (solid lines) and previously published data of dog brain tissues by Foster *et al.* [20] (∘ and ∗) at body temperature. Lines a and open circles (∘) are for gray matter and lines b and stars (∗) are for white matter.

TABLE V
COMPARISON OF VALUES FROM (3) AND (4) USING THE PARAMETERS LISTED IN TABLES I AND II, RESPECTIVELY, WITH THE EXPERIMENTAL DATA FOR GRAY MATTER AT 24 °C AT SOME SELECTED FREQUENCY POINTS. THESE POINTS ARE IN CURVES a OF FIGS. 5 AND 7. THE EXPERIMENTAL DATA AT 0.1, 1, AND 10 MHz ARE FROM [8] AT 24.5 °C. N/A STANDS FOR NOT APPLICABLE

	ϵ'			σ (S/m)		
frequencies (MHz)	value of Eq. (3)	value of Eq. (4)	experimental data	value of Eq. (3)	value of Eq. (4)	experimental data
0.1	N/A	2816	2806 ± 6	N/A	0.161	0.150 ± 0.020
1.0	N/A	1197	923 ± 3	N/A	0.202	0.177 ± 0.008
10.0	N/A	338	265 ± 5	N/A	0.356	0.295 ± 0.005
99.9	88.6	94.4	88.8 ± 8.6	0.765	0.671	0.764 ± 0.034
901.8	57.0	55.4	57.0 ± 3.0	1.06	1.13	1.04 ± 0.15
10179.8	45.0	44.6	44.6 ± 2.1	10.8	10.1	10.6 ± 0.8
26500.0	28.0	27.3	27.7 ± 2.2	33.0	34.9	36.1 ± 4.1

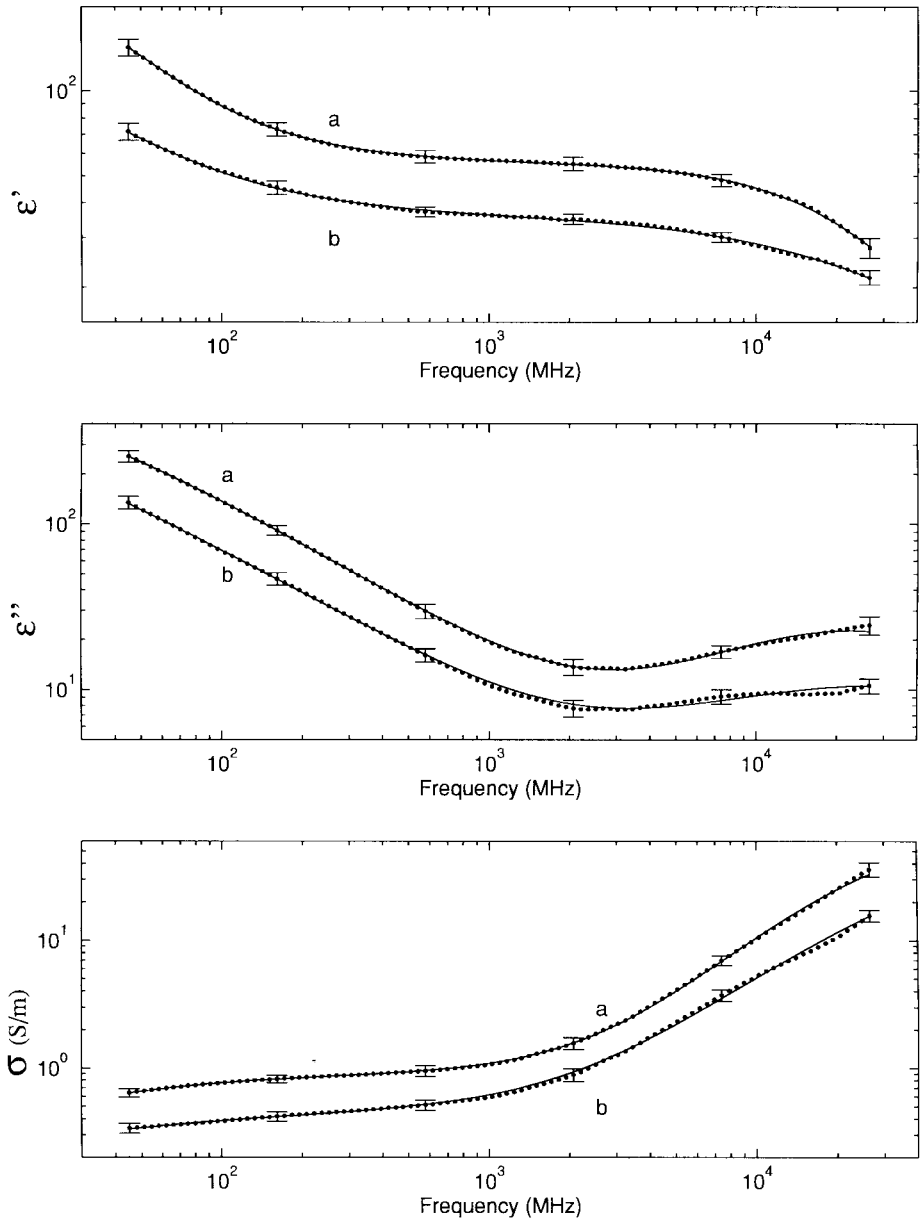

Fig. 5. Comparison between the measured data (•) and their CNLS fitting (solid lines) with (3). Curves a are for gray matter at 24 ± 0.5 °C while curves b are for white matter at 25 ± 0.5 °C. The best-fitted parameters are listed in Table I. The error bars stand for the standard deviations.

is that its inversion is unique so that no efforts were needed to distinguish the solutions and is much easier than that with a more complicated model.

B. Sample Preparation and Experimental Setup

Male Wistar–Kyoto rats were used as tissue donors. They were euthanized by CO_2 inhalation until the time of death. The brain and approximately 5 mm of the spinal cord were dissected free of skull and dura matter of the meninges in less than 10 min after death. The cerebral cortex consists of approximately a 2-mm-thick surface layer of gray matter and about a 6-mm-thick layer underneath a mixing region of gray and white matter. Since the gray matter was in direct contact with the open end of the probe and the measurement thickness into the specimen is about 2 mm [19], gray matter contributed the most to the measurements. Therefore, gray matter was used to represent the cerebral cortex. Medulla oblongata was constituted nearly solely by white matter and used to signify the white matter. Its thickness is about 7 mm. The specimens were washed with and immersed in 0.9% saline during the temperature adjusting process and measurements. Keeping the specimens in saline has the following advantages:

1) maintaining the tissues in a more physiologically friendly environment than in air;
2) making the temperature control easier;
3) avoiding any air bubbles which would possibly exist between the flat open end of the probe and the specimen surface if the specimen were kept in air.

Measurements at room temperature were done within 40 min, and at body temperature within 60 min after the euthanasia of

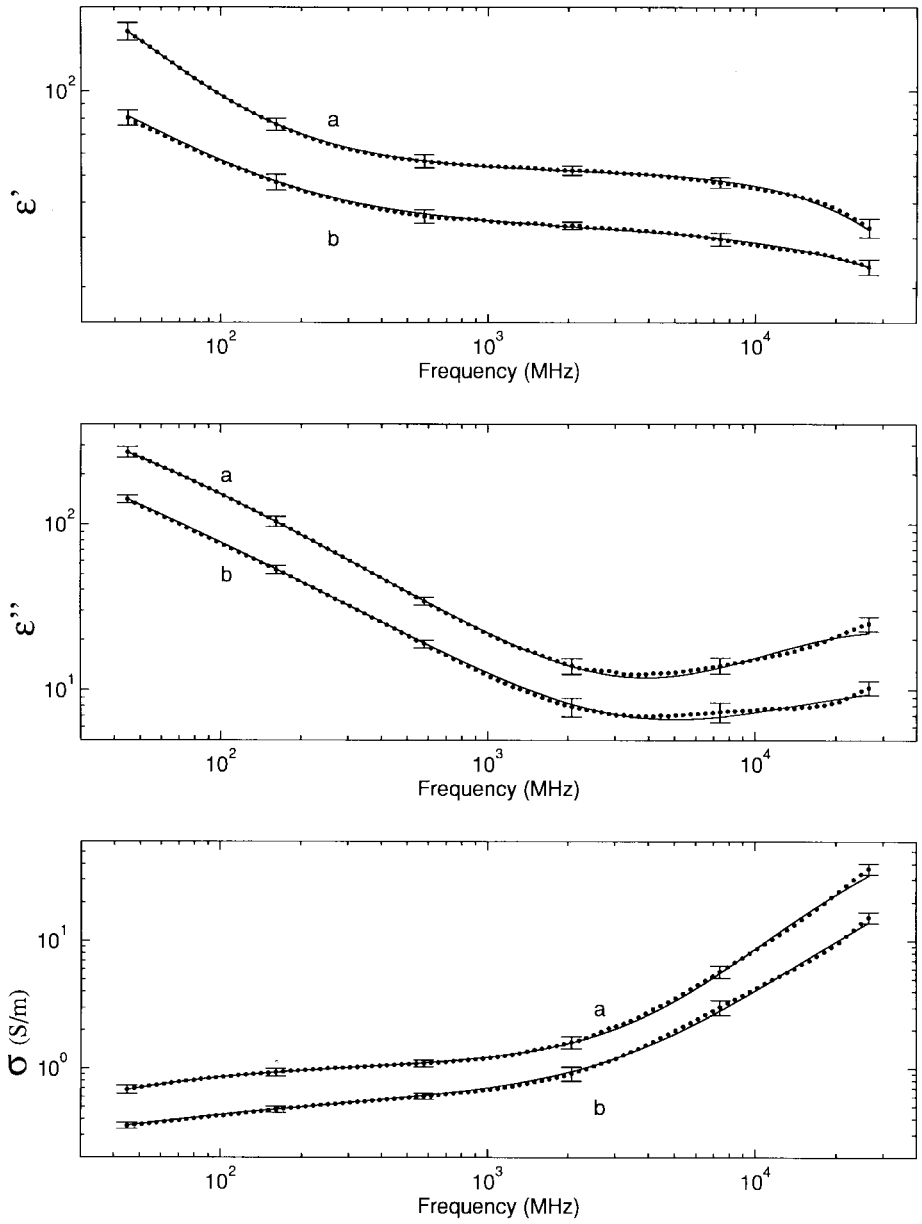

Fig. 6. Comparison between the measured data (•) and their CNLS fitting (solid lines) with (3) at 37 ± 0.5 °C. Curves a are for gray matter and curves b are for white matter. The best-fitted parameters are listed in Table I. The error bars stand for the standard deviations.

the rats. The whole brain tissue was kept intact, and one brain specimen was used only once at one temperature to ensure that the measurements were on fresh tissues. A total of 12 rat brains were utilized in this study. The probe position and the geometry of the sample container were kept the same during the saline reference and the tissue measurements to minimize environmental influences. The surface of specimens was in good and tight contact with the flat open-end of the probe. The measurement system is very similar to the one which has been described in [17], [18]. Measurements were done on the surface of specimens using an HP8510B network analyzer with a semirigid right-angle coaxial probe of 2.2-mm diameter and 15-cm length. Frequency range from 45 MHz to 26.5 GHz was swept on a logarithmic scale over 201 points in less than 1 min. The temperature was controlled by a water circulator, and measured on the surface of tissue specimens. Fig. 1 shows the tissue-probe configuration and measurement locations of a probe on the surface of a rat brain. The complex dielectric spectra were measured at different locations on the surface of specimen for gray and white matter, respectively.

III. Measurement Results

The dielectric properties of tissues in radio and microwave frequencies depend on their cellular and subcellular structures and constituents. Fig. 2 exhibits the measured permittivity (ϵ') and conductivity (σ) spectra of gray matter at 37 °C and 24 °C, and of white matter at 37 °C and 25 °C in the frequency range between 45 MHz and 26.5 GHz. σ is defined as $\sigma = \omega\epsilon_0\epsilon''$, where ϵ_0 is the permittivity in a vacuum, and ω is the angular frequency. Each of the spectra presents two well-separated major dispersions, which are commonly

TABLE VI
COMPARISON OF VALUES FROM (3) AND (4) USING THE PARAMETERS LISTED IN TABLES I AND II, RESPECTIVELY, WITH THE EXPERIMENTAL DATA FOR WHITE MATTER AT 25 °C AT SOME SELECTED FREQUENCY POINTS. THESE POINTS ARE IN CURVES b OF FIGS. 5 AND 7. THE EXPERIMENTAL DATA AT 0.1, 1, AND 10 MHz ARE FROM [8] AT 24.5 °C. N/A STANDS FOR NOT APPLICABLE

	ϵ'			σ (S/m)		
frequencies (MHz)	value of Eq. (3)	value of Eq. (4)	experimental data	value of Eq. (3)	value of Eq. (4)	experimental data
0.1	N/A	1365	1425 ± 25	N/A	0.106	0.150 ± 0.050
1.0	N/A	540	401 ± 1	N/A	0.125	0.120
10.0	N/A	165	120 ± 5	N/A	0.191	0.165 ± 0.005
99.9	51.5	56.2	51.8 ± 5.2	0.387	0.343	0.385 ± 0.060
901.8	36.5	35.9	36.4 ± 1.5	0.597	0.622	0.572 ± 0.075
10179.8	28.5	28.4	28.1 ± 1.2	5.23	4.89	5.37 ± 0.50
26500.0	21.6	21.9	21.7 ± 1.3	15.5	15.6	15.6 ± 1.6

referred to as β- and γ-dispersion [1], although only the high frequency tail of the β-dispersion is covered in this frequency range. The β-dispersion, centered in the megahertz frequency range, is largely due to the occurrence of Maxwell–Wagner effects at the interface between the cell membrane and the surrounding aqueous phase. The γ-dispersion, centered in the gigahertz frequency range, is attributed to the relaxation of water molecules in the aqueous phase or bound to macromolecules. Besides the long tails of β-dispersion, our spectra do not show a distinct so-called β'-dispersion. If it existed, it would be covered in our frequency range. Gray and white matter display a distinct dielectric property in this frequency range, where ϵ' and σ of gray matter constantly yield a higher value than those of white matter at both body and room temperatures, respectively. The temperature dependence of the spectra shows a crossing feature: ϵ' increases with temperature at low and high frequency ranges of this spectra and decreases in the middle, while σ increases with temperature in the low frequency range and decreases in the high frequency range. This feature is consistent with an earlier observation in a different cell system [18].

Fig. 3 illustrates a typical time-course of the measured ϵ' and σ spectra of grey matter at body temperature. Since the tissue samples were pressed against the probe, minor damage took place on their surface. The surface damage in turn caused a change of the interfacial properties with time. The systematic variation with time may be resulted from the leakage of the extracellular and intercellular fluid and/or elastic deformation of the tissues around the open-end of the probe, but not due to temperature variation, which shows a different feature (Fig. 2). To minimize the influence caused by the damage, a measurement should be performed as quickly as possible after a tissue specimen is placed in good contact with the probe.

Fig. 4 represents the comparison between the measured spectra of this paper and previously published data of a canine brain by Foster *et al.* [20] at 37 °C. Although our data constantly show a larger difference for both ϵ' and σ between gray and white matter, they are in reasonable agreement with the early data considering the factors such as using different measurement techniques and tissues from different species. One possible reason for the larger difference in our data is that we were using much fresher specimens. In addition, our spectra cover a wider frequency range.

IV. COMPLEX NONLINEAR ANALYSIS

To analyze these two well-separated dispersions, we need at least two dispersion functions. The measured spectra were analyzed using two models with and without considering previously published data at frequencies below 45 MHz, respectively. The adoption of early literature data in this modeling extends the valid frequency range of the model. The parameters of models are determined by means of a complex nonlinear least-squares (CNLS) fit, which simultaneously fits the real and imaginary parts to ensure a complete fit:

$$S(\vec{P}) = \sum_{k=1}^{N} \{W_k^r[\epsilon_m^r(\omega_k, \vec{P}) - \epsilon_e^r(\omega_k)]^2 + W_k^i[\epsilon_m^i(\omega_k, \vec{P}) - \epsilon_e^i(\omega_k)]^2\} \quad (2)$$

where N is the number of frequency points, ϵ_e is the experimental data, ϵ_m is given by an empirical model [see (3) or (4)], superscript r and i denote the real and imaginary parts, respectively, W is a weighting factor, and $\vec{P}$ represents the set of real parameters in the model. The best-fit values of these parameters are evaluated by minimizing S using the Levenberg–Margaret algorithm [21]. The procedure of our fitting routine can be found in [22].

The model utilized for the data solely from this paper contains two Cole–Cole functions:

$$\epsilon_m(\omega) = \epsilon_h + \frac{\Delta\epsilon_1}{1 + (j\omega\tau_1)^{\alpha_1}} + \frac{\Delta\epsilon_2}{1 + (j\omega\tau_2)^{\alpha_2}} + \frac{\sigma_0}{j\omega\epsilon_0} \quad (3)$$

where ϵ_h is the high-frequency limit of the dielectric constant, $\Delta\epsilon$ is the dielectric decrements of the dispersion, τ is the relaxation times, α are exponents, and σ_0 is the dc conductivity. The two Cole–Cole functions are for the two dispersions, and

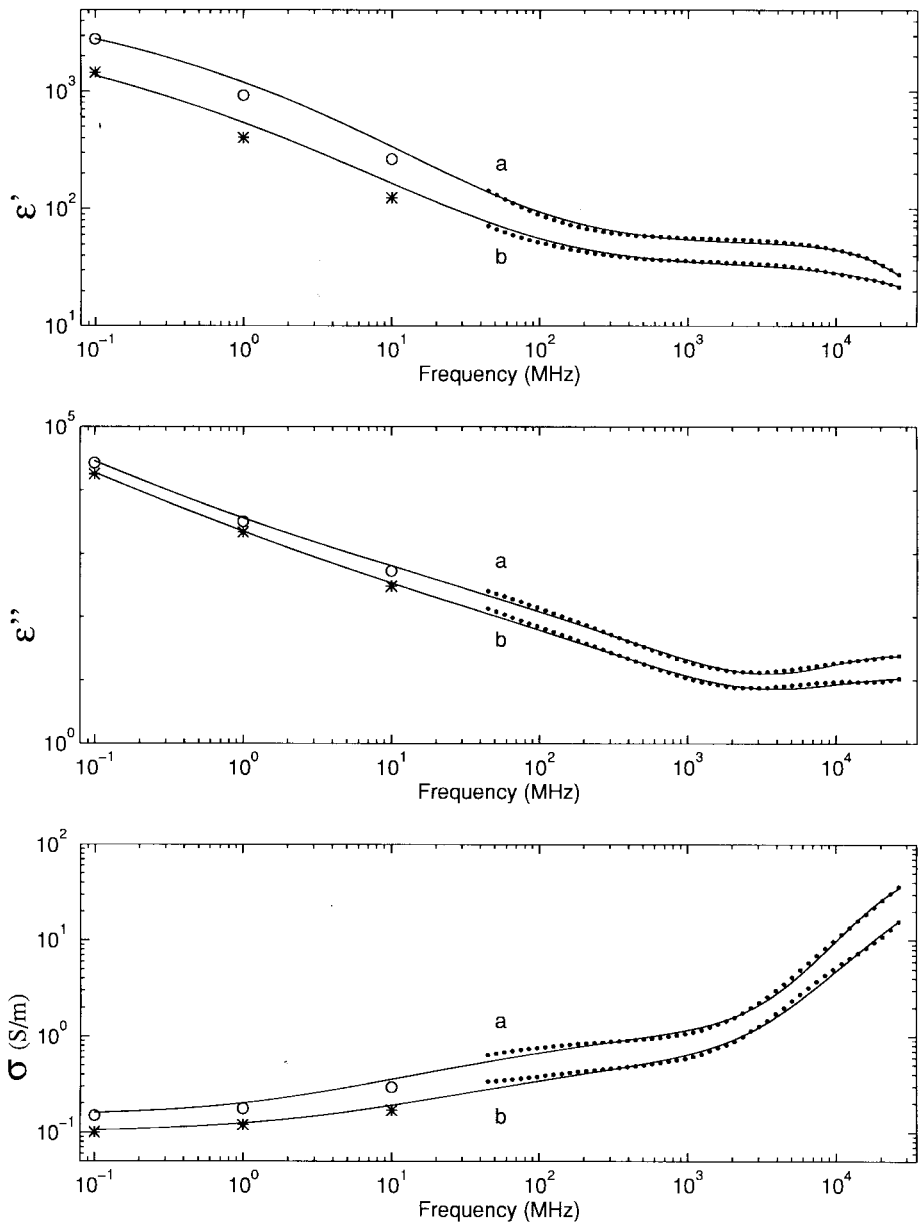

Fig. 7. Comparison between the measured data from this paper (•) plus previously published data of canine and bovine brain tissues at 24.5 °C by Surowiec *et al.* [8] (∘ and ∗) and the CNLS fitting (solid lines) with (4). Curves a and open circles (∘) are for gray matter and curves b and stars (∗) are for white matter. The best-fitted parameters are listed in Table II.

subscripts 1 and 2 represent the dispersions at low- and high-frequency ends, respectively. Since the data from this paper covers a very small portion of the β-dispersion, it is impossible to retrieve the entire β-dispersion from these data alone, and the parameters ($\Delta\epsilon_1$ and τ_1) obtained with the fitting do not reflect the β-dispersion. A large part of the γ-dispersion was in our measurement range so that the recovery of γ-dispersion is relatively more reliable. Nevertheless, we suggest that the extracted parameters in the model should only be used in the frequency range where the experimental data reside. Fig. 5 shows that the comparison between the measurement data and their CNLS fitting for gray and white matter at 24 °C and at 25 °C, respectively, and Fig. 6 shows a similar comparison at 37 °C. Only half of the measured data were plotted to make the fitting lines more visible in these two figures. Despite some small discrepancy in the imaginary part at high frequencies, (3) generally gives a good fit. The corresponding best-fitted parameters for (3) are listed in Table I.

Because the difference between the dielectric properties of the same organ but in different species is small [19], [23], and to the best of our knowledge there is no published low-frequency data (<45 MHz) for rat brains at the temperatures we were working with, we adopted the data of canine's gray and white matter at lower frequencies (10 MHz, 1 MHz, and 100 kHz) by Stoy *et al.* [7] at body temperature and Surowiec et al. [8] at room temperature. Utilizing the published data as references (even from different species) at frequencies below our measurement range in the fitting can increase the frequency range of validity of the model. There are only a few available published data for white and gray matter, regardless

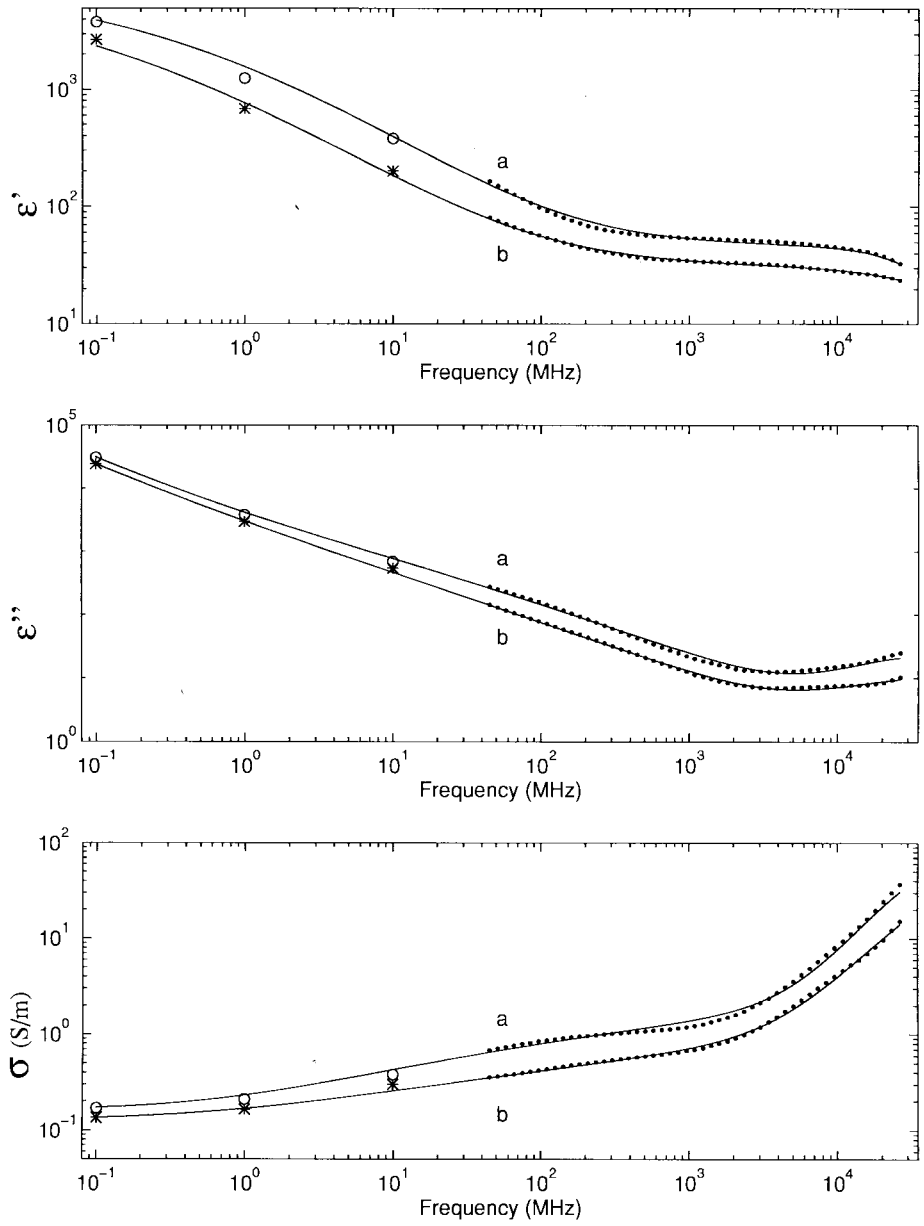

Fig. 8. Comparison between the measured data from this paper (•) plus previously published data of dog brain tissues by Stoy *et al.* [7] (∘ and ∗) and the CNLS fitting (solid lines) with (4) at 37 °C. Curves a and open circles (∘) are for gray matters and curves b and stars (∗) are for white matters. The best-fitted parameters are listed in Table II.

of the frequencies, temperatures, techniques, and species [2], [23], [24]. The extended dispersion at the low-frequency end was modeled with a Havriliak–Negami rather than Cole–Cole function to increase the flexibility of the model, and so (3) becomes

$$\epsilon_m(\omega) = \epsilon_h + \frac{\Delta\epsilon_1}{[1+(j\omega\tau_1)^{\alpha_1}]^{\beta_1}} + \frac{\Delta\epsilon_2}{1+(j\omega\tau_2)^{\alpha_2}} + \frac{\sigma_0}{j\omega\epsilon_0} \quad (4)$$

where β_1 is another exponent. Fig. 7 shows that the comparison between the combined data and their CNLS fitting for gray and white matter at room temperatures, while Fig. 8 shows a similar comparison at body temperature. Only one quarter of the measured data from this paper were plotted to make the fitting lines more visible. Although the quality of fit with (4) to the combined data is not as good as that with (3) to the present data, (4) covers a wider frequency range. The closest available room temperature data is at 24.5 °C [8], which is a half degree higher than our gray-matter temperature and a half degree lower than our white-matter temperature. The transition from our measured spectra to the early published data are fairly smooth for body temperature but less smooth for room temperature, which might be a partial result of the 0.5 °C difference between the temperatures at which the data were collected. The best-fitted parameters for the gray and white matter in the extended frequency range are listed in Table II. Since the combined data was applied to extract its best-fit parameters, (4) can be regarded for the *general* gray and white matter in the frequency range between 100 kHz and 26.5 GHz. Tables III and VI shows the comparison of calculated values from (3) and (4) using the parameters listed in Tables I and II, respectively, with the experimental data for gray and

white matter at body and room temperatures at several selected frequency points. These points are around curves a or b of Figs. 5–8, respectively. Although, in general, (3) presents a better values in a smaller frequency range, both (3) and (4) can yield reasonably close values to the measurement data if the experimental uncertainty are taken into account.

V. Conclusions

The complex dielectric spectra of gray and white matter of rat brains have been measured with the open-ended coaxial-probe technique in the frequency range between 45 MHz and 26.5 GHz at body and room temperatures. This paper's data have been analyzed with two Cole–Cole functions and a combination of early and current literature data has been analyzed with one Havriliak–Negami and one Cole–Cole function using CNLS technique in a frequency range from 100 kHz to 26.5 GHz. Furthermore, we explicitly show the time variation of the spectra due to the damage of the sample surface. Our data and models complement a few existing data, especially for the high frequencies above 10 GHz.

VI. Acknowledgments

The authors thank M. E. Belt and D. D. Cox for building the temperature control system, and P. J. Henry for help with the animals. Author J.-Z. Bao wishes to thank Prof. C. C. Davis for the data acquisition software. The views, opinions, and/or findings contained in this paper are those of the authors and should not be construed as an official Department of Army position, policy, or decision unless so designated by other documentation.

References

[1] K. R. Foster and H. P. Schwan, "Dielectric properties of tissues," in *Handbook of Biological Effects of Electromagnetic Fields*, C. Polk and E. Postow, Eds. New York: CRC, 1996, pp. 25–102.

[2] M. A. Stuchly, T. W. Athey, S. S. Stuchly, G. M. Samaras, and G. Taylor, "Dielectric properties of animal tissues in vivo at frequencies 10 MHz–1 GHz," *Bioelectromagnetics*, vol. 2, pp. 93–103, 1981.

[3] M. A. Stuchly and S. S. Stuchly, "Dielectric properties of biological substances—Tabulated," *J. Microwave Power*, vol. 15, pp. 19–26, 1980.

[4] C.-K. Chou, H. Bassen, J. Osepchuk, R. Petersen, M. Meltz, R. Cleveland, J. C. Lin, and L. Heynick, "Radio frequency electromagnetic exposure: Tutorial review on experimental dosimetry," *Bioelectromagnetics*, vol. 17, pp. 195–208, 1996.

[5] C.-K. Chou, "Evaluation of microwave hyperthermia applicators," *Bioelectromagnetics*, vol. 13, p. 581, 1992.

[6] C. J. F. Bottcher and P. Bordewijk, *Theory of Electric Polarization—Volume II*, 2nd ed. New York: Elsevier, 1978.

[7] R. D. Stoy, K. R. Foster, and H. P. Schwan, "Dielectric properties of mammalian tissues from 0.1 to 100 MHz: A summary of recent data," *Phys. Med. Bio.*, vol. 27, pp. 501–513, 1982.

[8] A. Surowiec, S. S. Stuchly, and A. Swarup, "Postmortem changes of the dielectric properties of bovine brain tissues at low radio-frequencies," *Bioelectromagnetics*, vol. 7, pp. 31–43, 1986.

[9] E. C. Burdette, F. L. Cain, and J. Seals, "In vivo probe measurement technique for determining dielectric properties at VHF through microwave frequencies," *IEEE Trans. Microwave Theory Tech.*, vol. MTT-28, pp. 414–427, Apr. 1980.

[10] T. W. Athey, M. A. Stuchly, and S. S. Stuchly, "Measurement of radio frequency permittivity of biological tissues with an open-ended coaxial line: Part I." *IEEE Trans. Microwave Theory Tech.*, vol. MTT-30, pp. 82–86, Jan. 1982.

[11] M. A. Stuchly, A. W. Athey, G. M. Samaras, and G. E. Taylor, "Measurement of radio frequency permittivity of biological tissues with an open-ened coaxial line: Part II—Experimental results," *IEEE Trans. Microwave Theory Tech.*, vol. MTT-30, pp. 87–92, Jan. 1982.

[12] L. L. Li, B. Ismail, L. S. Taylor, and C. C. Davis, "Flanged coaxial microwave probes for measuring thin moisture layers," *IEEE Trans. Bio-Med. Eng.*, vol. 39, pp. 49–57, Jan. 1992.

[13] C. Gabriel, T. Y. A. Chan, and E. H. Grant, "Admittance models for open ended coaxial probes and place in dielectric spectroscopy," *Phys. Med. Biol.*, vol. 39, pp. 2183–2200, 1994.

[14] S. Bringhurst and M. F. Iskander, "Open-ended metallized ceramic coaxial probe for high-temperature dielectric properties measurements," *IEEE Trans. Microwave Theory Tech.*, vol. 44, pp. 926–935, June 1996.

[15] G. Q. Jiang, W. H. Wong, E. Y. Raskovich, W. G. Clark, W. A. Hines, and J. Sanny, "Open-ended coaxial-line technique for the measurement of the microwave dielectric constant for low-loss solids and liquids," *Rev. Sci. Instrum.*, vol. 64, pp. 1614–1621, June 1993.

[16] J. Baker-Jarvis, M. D. Janezic, P. D. Domich, and R. G. Geyer, "Analysis of an open-ended coaxial probe with lift-off for nondestructive testing," *IEEE Trans. Instrum. Meas.*, vol. 43, pp. 711–718, Oct. 1994.

[17] J.-Z. Bao, C. C. Davis, and M. L. Swicord, "Microwave dielectric measurements of erythrocyte suspensions," *Biophys. J.*, vol. 66, pp. 2173–2180, 1994.

[18] J.-Z. Bao, M. L. Swicord, and C. C. Davis, "Microwave dielectric characterization of binary mixtures of water, methanol, and ethanol," *J. Chem. Phys.*, vol. 104, pp. 4441–4450, 1996.

[19] M. A. Stuchly, K. A. Stuchly, and A. M. Smith, "Dielectric properties of animal tissues in vivo at radio and microwave frequencies: comparison between species," *Phyiscs in Medicine and Biology*, vol. 27, pp. 927–1159, 1982.

[20] K. R. Foster, J. L. Schepps, R. D. Stoy, and H. P. Schwan, "Dielectric properties of brain tissue between 0.01 and 10 GHz," *Phys. Med. Biol.*, vol. 24, pp. 1177–1187, 1979.

[21] W. H. Press, B. P. Flannery, S. A. Teukolsky, and W. T. Vetterling, *Numerical Recipes in C*, 2 ed. Cambridge, U.K.: Cambridge Univ. Press, 1992.

[22] J.-Z. Bao, C. C. Davis, and R. E. Schmukler, "Impedance spectroscopy of human erythrocytes: System calibration and nonlinear modeling," *IEEE Trans. Bio-Med. Eng.*, vol. 40, pp. 364–378, Apr. 1993.

[23] J. C. Lin, "Microwave properties of fresh mammalian brain tissues at body temperature," *IEEE Trans. Bio-Med. Eng.*, vol. BME-22, pp. 74–76, Jan. 1975.

[24] N. R. V. Nightingale, A. W. J. Dawkins, R. J. Sheppard, E. H. Grant, V. D. Goodridge, and J. L. Christie, "The use of time domain spectroscopy to measure the dielectric properties of mouse brain at radiowave and microwave frequencies," *Phys. Med. Biol.*, vol. 25, pp. 1161–1165, 1980.

Jian-Zhong Bao (M'92–SM'96) was born in Beijing, China, in 1958. He received the B.S. degree in physics from Northwestern University, Xian, China, in 1982, and the Ph.D. degree in chemical physics from the University of Maryland at College Park (UMCP), in 1991.

From 1982 to 1985, he was a Faculty Member at Xidian University, Xian, China. From 1986 to 1991, he was a Graduate Research Assistant in the Department of Electrical Engineering, UMCP, working on electrical impedance measurements and modeling of red-blood cells in the frequencies from 1 Hz to 10 MHz, membrane phase transition, and electrical-field simulation, and from 1992 to 1994, he was a Research Associate, working on dielectrometry of macromolecules, binary solutions of simple molecules, and simple cellular systems in gigahertz range. Since 1994, he has been with McKesson BioServices, as a Senior Research Engineer with the U.S. Army Medical Research Detachment, Brooks Air Force Base, San Antonio, TX. He has been working on various projects that include signal processing of picosecond electromagnetic pulses and electromagnetic simulation with the finite-difference time-domain method. His current research interest is the application of object-oriented methodologies to electromagnetic modeling. He has authored over 20 publications in the areas of impedance and microwave dielectric measurements and characterization of materials, measurements and signal processing of electromagnetic pulses, and computer simulation of electromagnetics.

Dr. Bao is a member of the American Physical Society, Bioelectromagnetics Society, Biophysical Society, and Computer Society, and his name is listed in *American Men and Women of Science* and *Who's Who in Science and Engineering*.

Shin-Tsu Lu was born in Taipei, Taiwan, R.O.C., in 1943. He received the B.V.M. degree in veterinary medicine in 1968 from National Taiwan University, Taipei, and the M.S. and Ph. D. degrees in radiation biology from the University of Rochester, Rochester, NY, in 1973 and 1977, respectively.

From 1972 to 1990, he served as a Staff and Faculty Member at the University of Rochester, School of Medicine, Department of Medicine, Cardiology Unit, Department of Radiation Biology and Biophysics, Aerosol Research Laboratory, and Department of Biophysics. He also served as a Scientific Consultant to various private and governmental research laboratories and a Scientific Reviewer on publication and grant applications. Since 1990, he has been the Senior Research Physiologist of the McKesson BioServices at the U.S. Army Medical Research Detachment, Microwave Bioeffects Branch at Brooks AFB, San Antonio, TX. His research has concentrated on biological effects of radio-frequency radiation and ELF fields.

Dr. Lu is a member of the Bioelctromagnetics Society, Engineering in Medicine and Biology Society, and ANSI C95.4.

William D. Hurt (SM'78) was born in Georgetown, TX, on March 16, 1942. He received the B.S. degree and the M.S. degree in physics from St. Mary's University, San Antonio, TX, in 1964 and 1971, respectively, and the M.S. degree in engineering from the University of Texas at Austin, in 1976.

He is a Research Physicist at the Armstrong Laboratory, Brooks Air Force Base, San Antonio.

Mr. Hurt is a member of the IEEE Standards Coordinating Committee 28, Subcommittee I, Techniques, Procedures, and Instrumentation.